

Supplementary Figure 1. Mutant library design.

- A, B.** Uniform coverage of mutations along synthetic genes in the small library (**A**) and big library (**B**).
C. Distributions of the number of single nucleotide substitutions per gene (upper panels) and of substitutions+deletions+insertions per gene (lower panels) in the two mutant libraries.

Supplementary Figure 2. Complementation of D343 strain with U3.

Growth of D343 cells supplemented with wild-type U3 (top panels), empty plasmid (middle panels) or a non-functional mutant of U3 (mutation list: C43T, C75G, A169C, G202T, G248C, C252T, C259T, G282T, A293T, T302A, G302A, G305del; bottom panels) on glucose and galactose media without adenine.

Supplementary Figure 3. Reproducibility of fitness measurements.

- A.** Reproducibility of fitness measurements for individual barcodes in experiments Small_1_30C_Glu (X axis) and Small_3_30C_Glu (Y axis). R= 0.78.
B. Reproducibility of mean fitness per site (f_i) in experiments Small_1_30C_Glu (X axis) and Small_3_30C_Glu (Y axis). R=0.92.
C. Reproducibility of fitness measurements among high-coverage variants. The mean and standard deviation of log fitness are shown for 824 variants with at least two measurements with 1000 or more reads in population G0 among datasets Small_1_30C_Glu and Small_3_30C_Glu.

Supplementary Figure 4. Effects of mutations on folding energy.

- A.** Nomenclature of stems in the secondary structure of U3. Yeast-specific regions are shown in blue, regions conserved among Eukaryotes are in red.
B. The mean fitness of U3 variants binned by ascending minimal folding energy, calculated separately for each stem and for hinge-pre-rRNA hybrids. Bin ranges (from left to right, for stems I, II and VI): bin 1, $\Delta\Delta G < 0$; bin 2, $\Delta\Delta G = 0$; bin 3, $0 < \Delta\Delta G < 1$; bin 4, $1 < \Delta\Delta G < 2$; bin 5,

$2 < \Delta\Delta G < 3$; bin 6, $\Delta\Delta G > 3$; for stems III, IV, V, 5' hinge and 3' hinge: bin 1, $\Delta\Delta G < 0$; bin 2, $\Delta\Delta G = 0$; bin 3, $0 < \Delta\Delta G < 2$; bin 4, $2 < \Delta\Delta G < 4$; bin 5, $4 < \Delta\Delta G < 6$; bin 6, $\Delta\Delta G > 6$. $\Delta\Delta G$ is the folding energy of the focal mutant minus the folding energy of the wild-type variant.

Supplementary Figure 5. Examples of fitness effects at specific sites.

Fitness effects of each type of mutation (substitutions to A, C, G, T and deletion) at position U191 (A) and positions in terminal stem (B- D).

Supplementary Figure 6. Comparison of fitness effects in 30C and 37C.

A-C, Distribution of p_i , the aggregate log fitness effect of position i across all genetic backgrounds, mapped to the U3 structure for individual experiments: Small_1_30C_Glu (**A**), Small_3_30C_Glu (**B**), and Small_2_37C_Glu (**C**). Arrows indicate positions in which the fitness effects were most different between 30C and 37C.

D-F, Scatter plots of p_i values between pairs of individual experiments.

Supplementary Figure 7. Alternative calculation of the fitness effects of mutations.

The aggregate log fitness effect of each position in experiment Small_1_30C_Glu was calculated as in Fig. S6, except that the median fitness effect of mutations was used instead of the mean, to correct for effects of outliers.

Supplementary Figure 8. Systematic bias of w_i estimated by ridge regression.

A-C, Comparison of single-site effects estimated directly from single mutants (X axis, f_i) and estimated by ridge regression (Y axis, w_i). (A,D), mean of Small_1_30C_Glu and Small_3_30C_Glu; (B,E), Small_2_37C_Glu; (C,F) Big_1_30C_Glu.

D-F, Bias in single-site effects estimated by ridge regression. Regression overestimates f_i for low-effect sites, and underestimates f_i for large-effect sites. To estimate the epistatic effects w_{ij}

by ridge regression, we therefore used empirical estimates of single-site effects from variants mutated at one position only (f_i).

Supplementary Figure 9. Maps of epistatic interactions calculated for individual datasets.

A, mean of Small_1_30C_Glu and Small_3_30C_Glu;

B, Small_2_37C_Glu

C, Big_1_30C_Glu

Supplementary Figure 10. Prediction of U3 secondary structure using constraints from positive epistasis.

A, Map of known basepairing contacts (top left), and of contacts inferred from filtered positive epistatic interactions (bottom right, see Methods). Known contacts are circled.

B, Minimum Folding Energy (MFE) secondary structure predicted by Vienna using U3 sequence data alone.

C, MFE structure predicted by Vienna using U3 sequence and the following basepairing constraints: 330-77 (epistasis score=0.30, epistasis rank=2), 331-76 (score=0.30, rank=3), 332-75 (score=0.23, rank=4), 50-60 (score=0.23, rank=5), 49-61 (score=0.22, rank=6). This structure is markedly more similar to the known structure than structure predicted from sequence alone. In particular, the terminal stem and Stem 2 are now correctly folded. Using centroid instead of MFE structures led to similar results.

Supplementary Figure 11. Cluster of negative epistatic interactions sis in the 3' hinge.

A, Enrichment in negative epistatic interactions in the “3’ hinge” (positions 62-73), which mediates basepairing of U3 with pre-rRNA.

B, The mean fitness (left axis) and U3-pre-rRNA interaction energy (right axis) of mutants binned by numbers of mutations in the 3’ hinge.

Supplementary Table 1. List of experiments.

Experiment name	Sample ID*	Time (h)†	Number of reads used	Number of barcodes recognised	Number of mutants accepted
Small_1_30C_Glu	total		76505765	41617	22372
	G0	0	14233050		
	D1.25	36	14051955		
	D2.25	60	11881307		
	D3.25	84	15850703		
	D4.25	108	20488750		
Small_2_37C_Glu	total		88384609	40250	23915
	G0	0	14013114		
	D1.25	36	14338456		
	D2.25	60	14277184		
	D3.25	84	14327688		
	D4.25	108	14365043		
	D5.25	132	2699207		
	D6.25	156	14363917		
Small_3_30C_Glu	total		201446365	41266	23163
	G0	0	28745264		
	D0.25	12	28843586		
	D0.75	24	28537727		
	D1.25	36	29034201		
	D2.25	60	28822264		
	D3.25	84	28646717		
	D4.25	108	28816606		
Small_3_30C_Gal	total		165773130	41509	23167
	G0	0	28745264		
	G0.25	12	21662238		
	G1.25	36	28813189		
	G2.25	60	28856414		
	G3.25	84	28866443		
	G4.25	108	28829582		
Big_1_30C_Glu	total		13622683	67069	36692
	G0	0	3488092		
	D0.25	12	2629826		
	D0.75	24	3083151		
	D1.25	36	4421614		

*The Sample ID represents the growth medium (G for galactose, D for glucose), and the duration of selection (in days) that was assumed for that sample in the fitness estimation. For example D1.25 represents a sample that was under selection on glucose for 1.25 days (30 hours). There is a 6-hour difference between the selection time and wall-clock time, because it took approximately 6 hours for genetically encoded U3 to be depleted after addition of glucose.

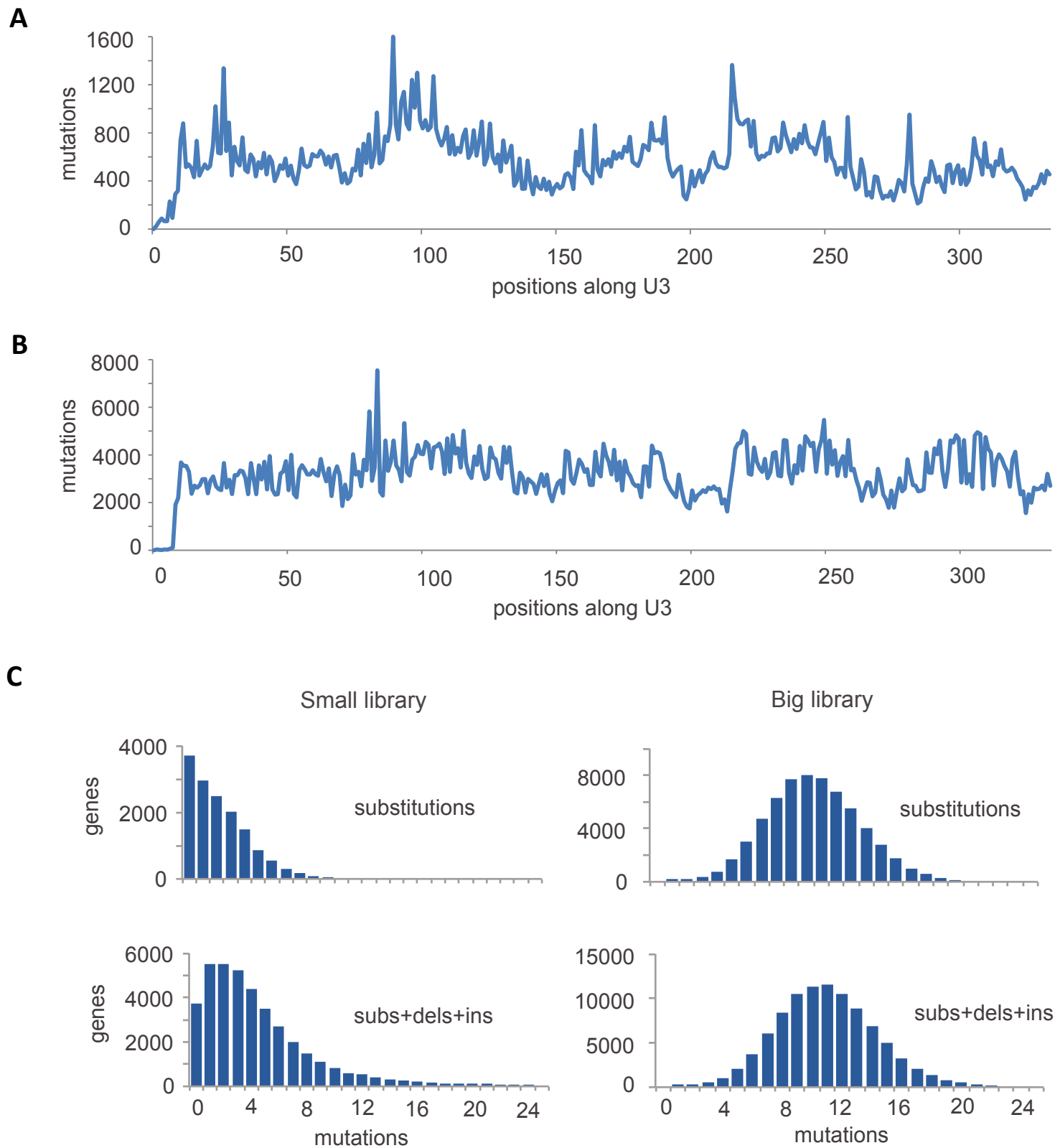
†Wall-clock time when sample was taken.

Supplementary Table 2. Sequences of oligonucleotides.

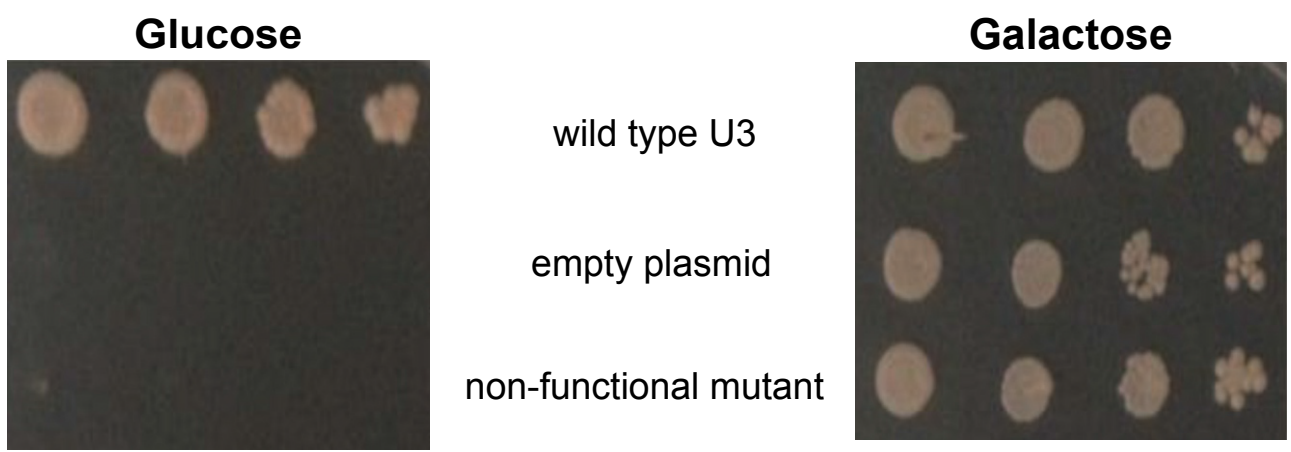
Name	Sequence
U3_1F_wt	CTTAAAATCTGTGTCGACGTACTCATAGGATCATTCTATA GAATCGTCACTCTTGACTCTCAAAAGAGCCACTGAATCCA ACTTGGTTGATGAGT
U3_1R_wt	ATTGCGGACCAAGCTAATTAGATTCAATT CGGTTCTCACT CTGGGGTACAAAGTTATGGGACTCATCAACCAAGTTGGA
U3_2F_wt	AAATTAGCTTGGTCCGCAATCCTAGCGGTCGGCCATCTATA ATT TTGAATAAAAATT TGCTTGCCGTTGCATT GTAGT
U3_2R_wt	AGTACATAGGATGGGTCAAGATCATCGGCCATAAAATATTG TAATTACTTCAAAGGAAAAACTACAATGCAACGGCAAA
U3_3F_wt	CTTGACCCATCCTATGTACTCTTTGAAGGGATAGGGCTC TATGGGTGGGTACAAATGGCAGTCTGACAAGTTAACAC
U3_3R_wt	TAATCCAATTCTTAACTGAAAACCAAACCTTGGTTAAAC AATTAGAAAAGGAAAAAGTGGTTAACTTGTCA GACT
U3_1F_mut	CTTAAAATCTGTGTCGACG(01019701)(01010197)(97010101)(019 70101)(01010197)(01010197)(01970101)(97010101)(01010197)(97010 101)(01019701)(01019701)(97010101)(01010197)(01970101)(9701010 1)(01010197)(01010197)(01010197)(01970101)(01010197)(97010101) (01010197)(97010101)(01019701)(01010197)(97010101)(97010101)(0 1010197)(01019701)(01019701)(01010197)(01970101)(01010197)(0101019 7)(01970101)(97010101)(01010197)(01970101)(01010197)(0101019 7)(01970101)(97010101)(97010101)(97010101)(97010101)(01019701) (97010101)(01019701)(01019701)(01010197)(01970101)(01010197)(019 70101)(01019701)(97010101)(97010101)(01010197)(01970101)(0101019 70101)(97010101)(97010101)(01010197)(01010197)(01010197)(0101019 70101)(01010197)(01010197)(01010197)(01010197)(01010197)(0101019 7)(01010197)(01010197)(01010197)(01010197)(01010197)(01010197)
U3_1R_mut	(97010101)(01010197)(01010197)(01019701)(01970101)(01019701)(0 1019701)(97010101)(01970101)(01970101)(97010101)(97010101)(010 19701)(01970101)(01010197)(97010101)(97010101)(01010197)(0101019 7)(01010197)(97010101)(97010101)(01010197)(01010197)(01010197) (01970101)(01019701)(01019701)(01010197)(01010197)(01010197)(010 1970101)(01010197)(01970101)(97010101)(01970101)(01010197)(0101019 70101)(01010197)(01010197)(01010197)(01010197)(01010197)(01010197) (01970101)(01970101)(97010101)(97010101)(01010197)(01010197)(0101019 70101)(01010197)(01010197)(01010197)(01010197)(01010197)(01010197)

	1019701)(97010101)(01970101)(97010101)(97010101)(01019701)(010197)(01010197)(97010101)(97010101)(01970101)(01970101)(97010101)(01970101)
U3_3R_mut	TAATCCAATTCTTAAC TGAAAACCAACCTTGGTTTAAAC AATTAGAAAAGGAAAAAGTGGTTA(97010101)(01970101)(010197)(01010197)(01019701)(01010197)(01970101)(97010101)(01019701)(01970101)(01010197)
U3_end_bar_EcoR1	ACGTACGN>NNNNNNNNNNNNNNNNNTAATCCAATTCTT AACTGA
U3_start_SalI	TTAAAATCTGTGTCGACG
EcoRI.oligo_SalI	ACGTACGTGAATTCACGTACGTACGTACGTACGTAC GT
SalI.oligo_EcoRI	ACGTACGTGTCGACACGTACGTACGTACGTACGTAC GT
Index1_PCR_U3_seq	CAAGCAGAACGGCATACGAGATATCATGAGTCAGTCAGC CTGTTCTACTTAAAATCTGT
Index2_PCR_U3_seq	CAAGCAGAACGGCATACGAGATCAAGTTAGTCAGTCAGC CTGTTCTACTTAAAATCTGT
R_PCR_U3bar_seq	AATGATA CGGC GACC ACCGAG ATCTAC ACTATGGTA ATTGTA AACGACGGCCAGTGAATT
Index1_PCR_bar_seq	CAAGCAGAACGGCATACGAGATCGTGATGTGACTGGAGTT CAGACGTGCTCTCCGATCTTCAGTTAAGAAATTGG
Index2_PCR_bar_seq	CAAGCAGAACGGCATACGAGATACATCGGTGACTGGAGT TCAGACGTGCTCTCCGATCTTCAGTTAAGAAATTGG
Index3_PCR_bar_seq	CAAGCAGAACGGCATACGAGATGCCTAAGTGACTGGAGT TCAGACGTGCTCTCCGATCTTCAGTTAAGAAATTGG
Index4_PCR_bar_seq	CAAGCAGAACGGCATACGAGATTGGTCAGTGACTGGAGTT CAGACGTGCTCTCCGATCTTCAGTTAAGAAATTGG
Index5_PCR_bar_seq	CAAGCAGAACGGCATACGAGATCACTGTGACTGGAGTT CAGACGTGCTCTCCGATCTTCAGTTAAGAAATTGG
Index6_PCR_bar_seq	CAAGCAGAACGGCATACGAGATATTGGCGTGACTGGAGTT CAGACGTGCTCTCCGATCTTCAGTTAAGAAATTGG
Custom_Read1_seq_p	TATGGTAATTGTAAACGACGGCCAGTGAATT

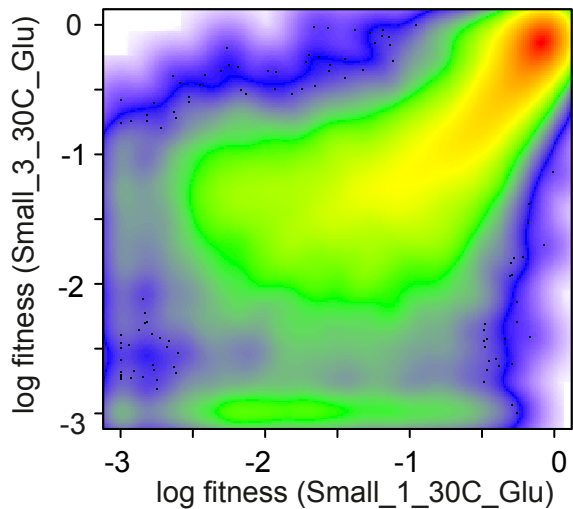
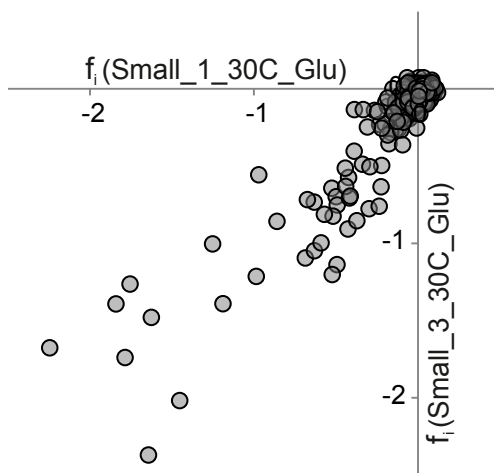
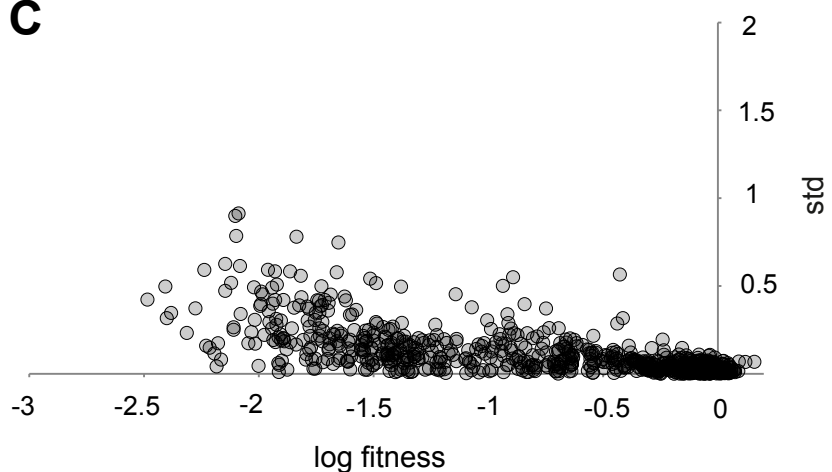
rimer_U3	
Proton_A_PCR_bar_s eq_F	CCATCTCATCCCTGCGTGTCTCCGACTCAGGTTTCAGTTAAG AAATTGG
Proton_A_PCR_bar_s eq_R	CCATCTCATCCCTGCGTGTCTCCGACTCAGTTGTAACGACG GCCAGTG
Proton_trP1_PCR_ba r_seq_F	CCTCTCTATGGGCAGTCGGTGATGTTTCAGTTAAGAAATTGG
Proton_trP1_PCR_ba r_seq_R	CCTCTCTATGGGCAGTCGGTGATTGTAAAACGACGGCCAGT G



Supplementary Figure 1
Puchta et al.

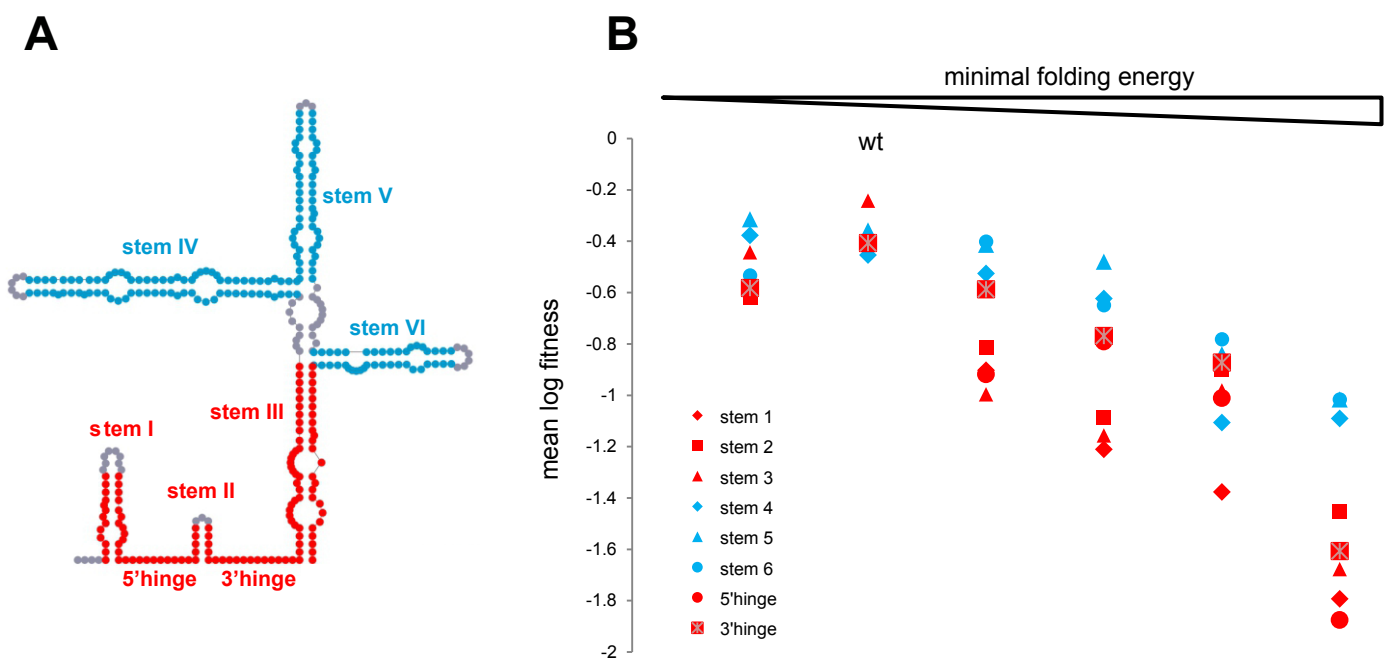


Supplementary Figure 2
Puchta et al.

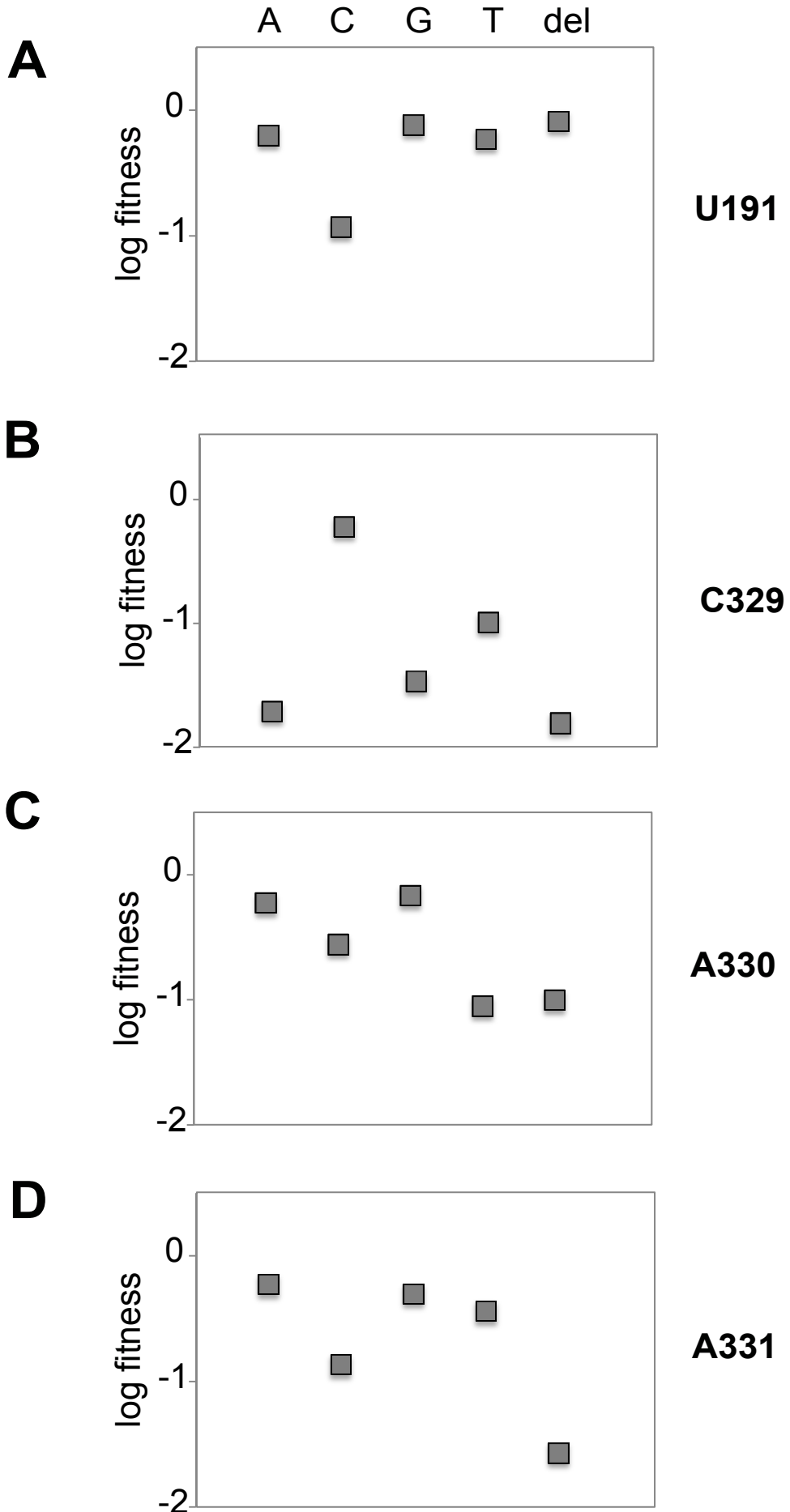
A**B****C**

Supplementary Figure 3

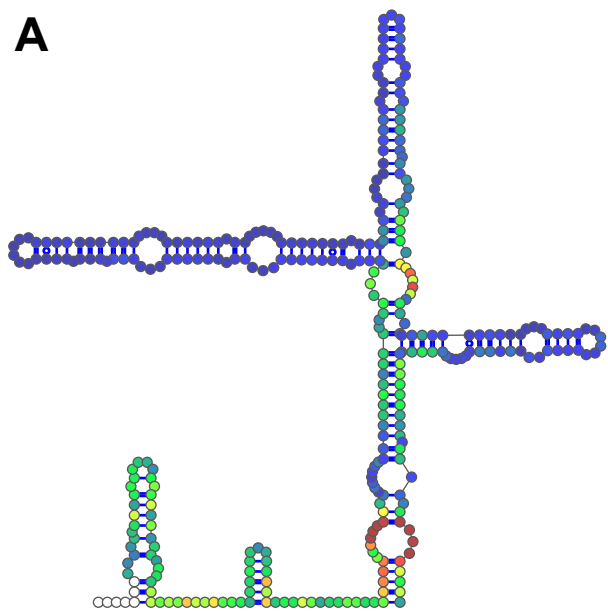
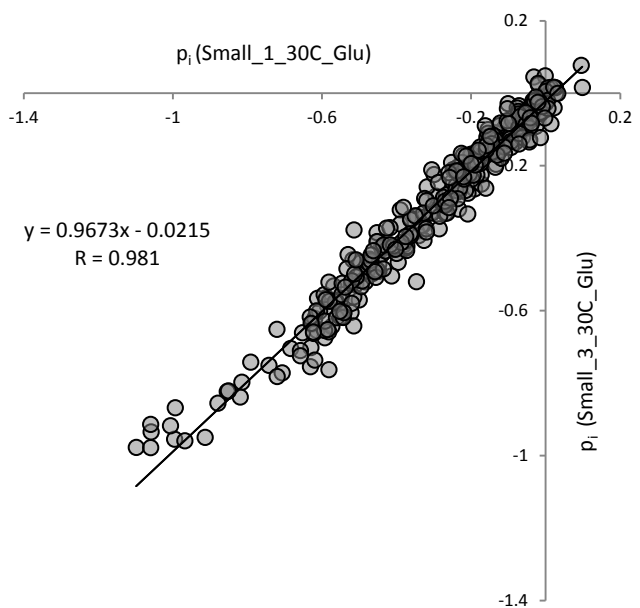
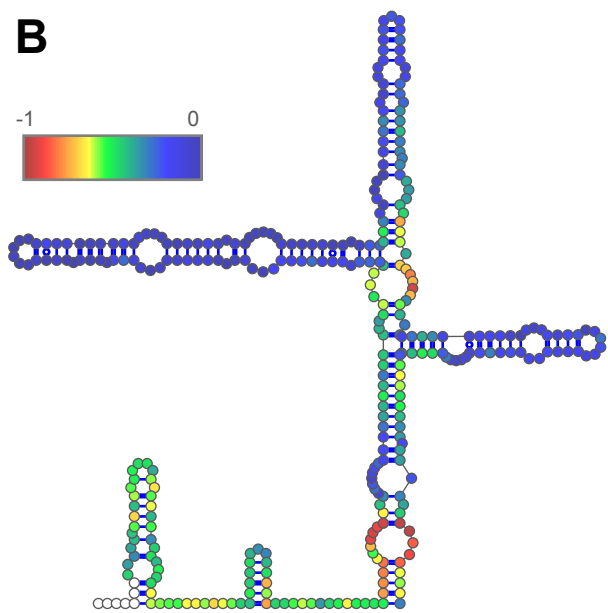
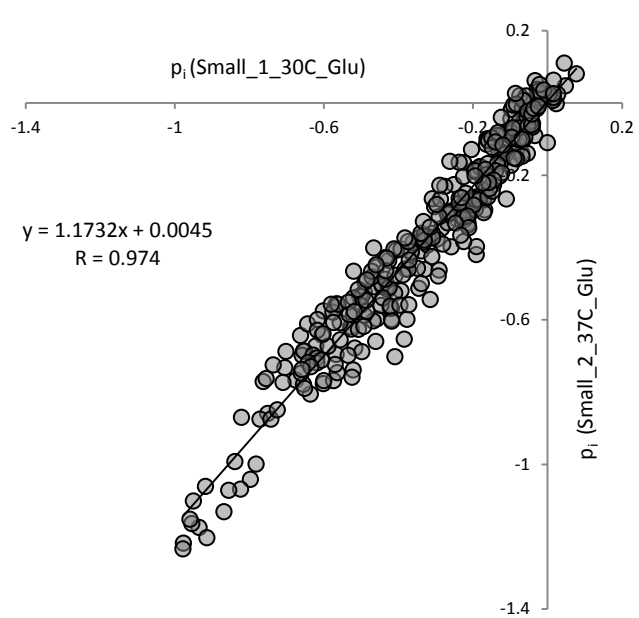
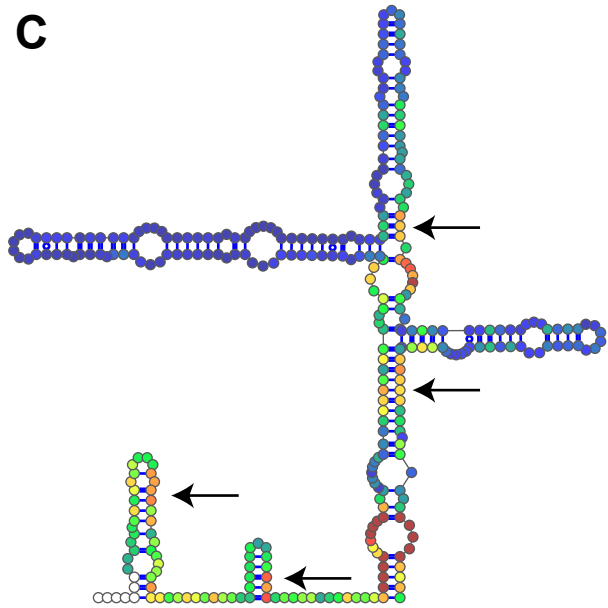
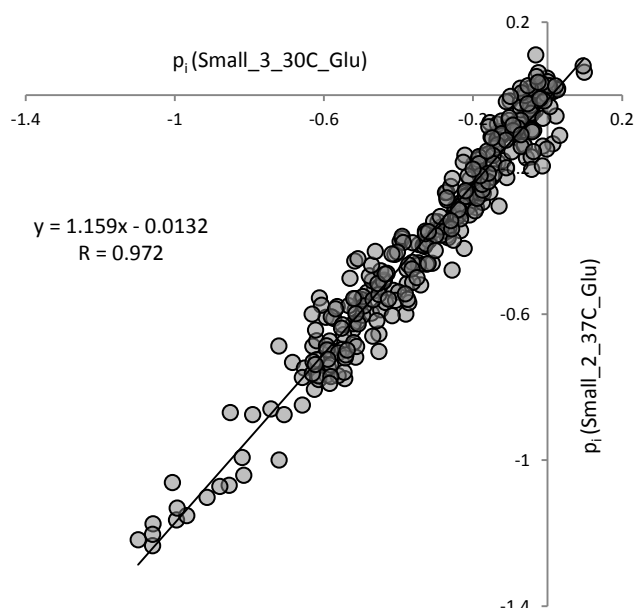
Puchta et al.



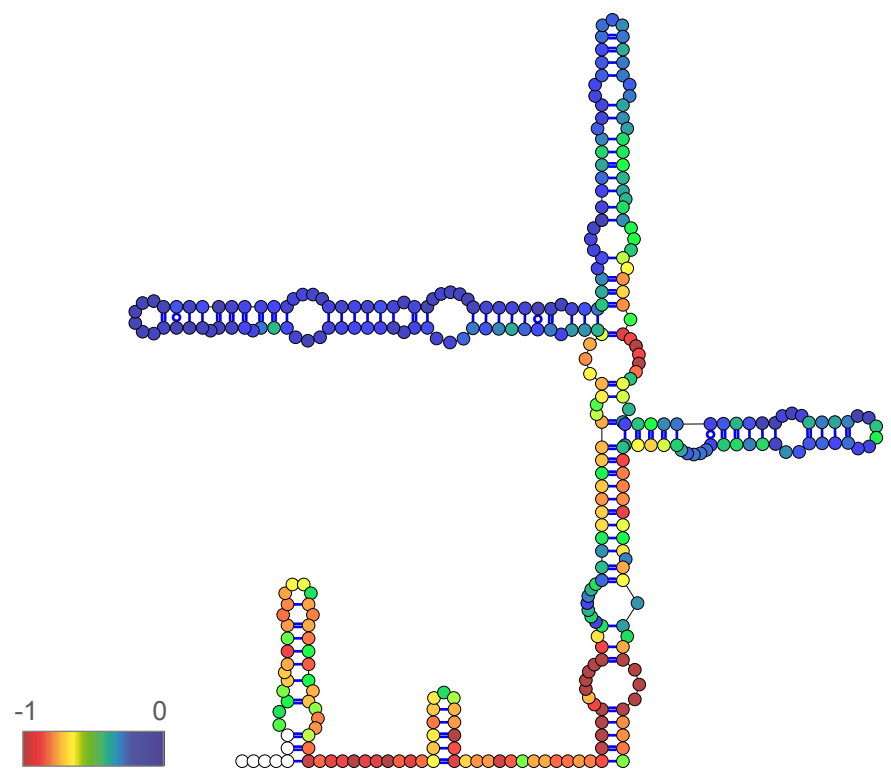
Supplementary Figure 4
Puchta et al.



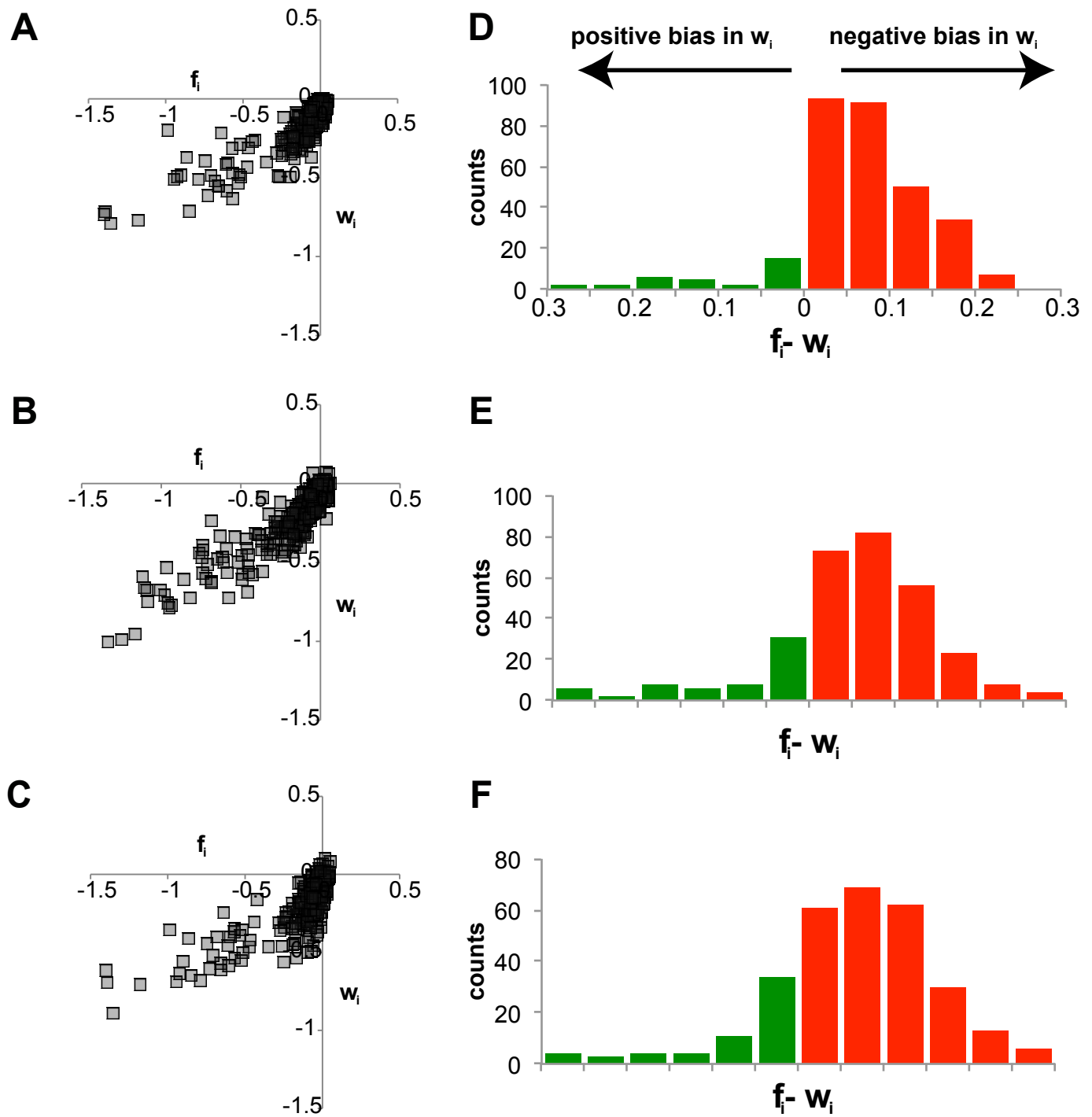
Supplementary Figure 5
Puchta et al.

A**D****B****E****C****F**

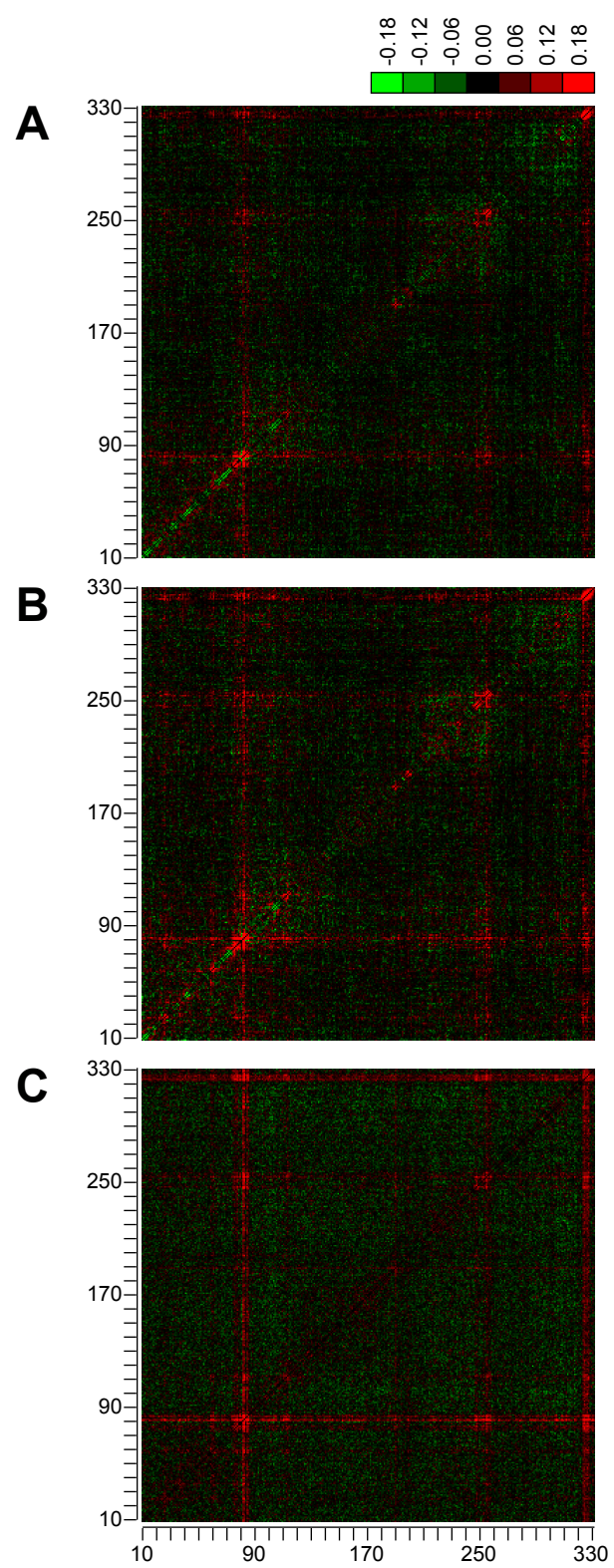
Supplementary Figure 6
Puchta et al.



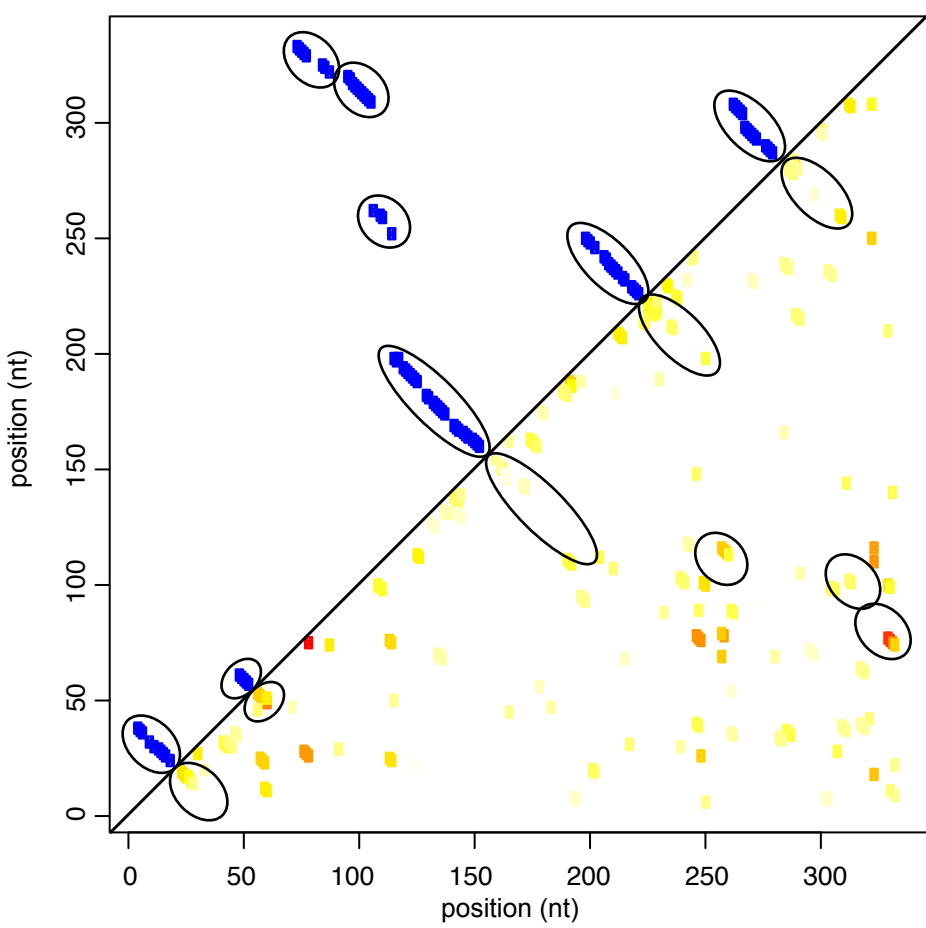
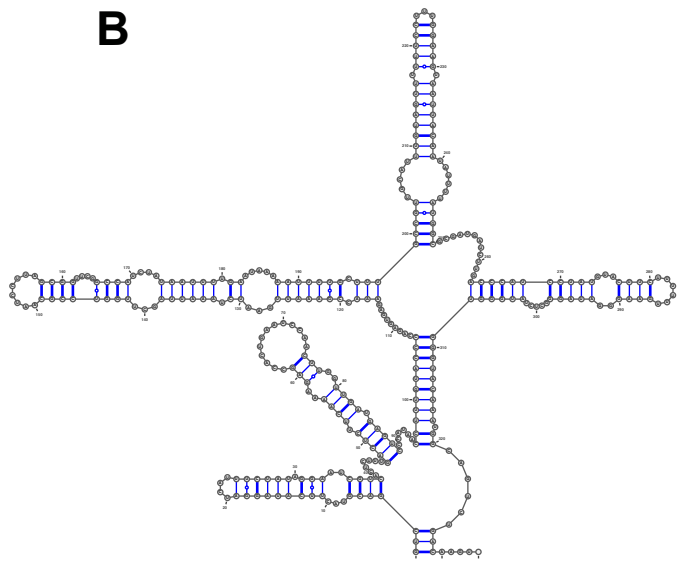
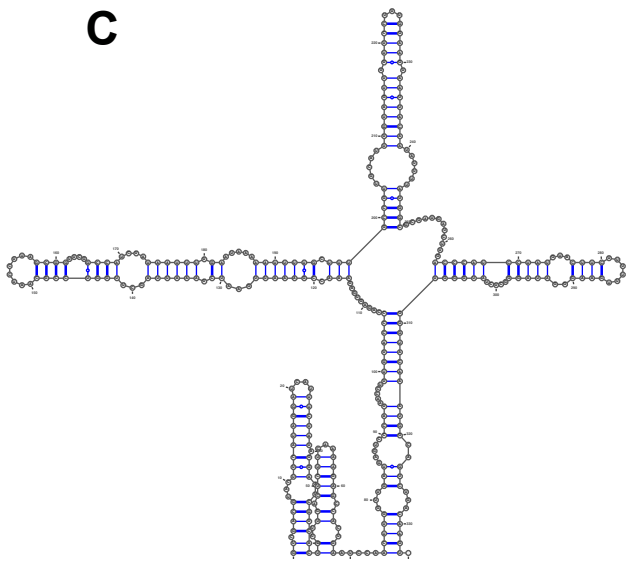
Supplementary Figure 7
Puchta et al.



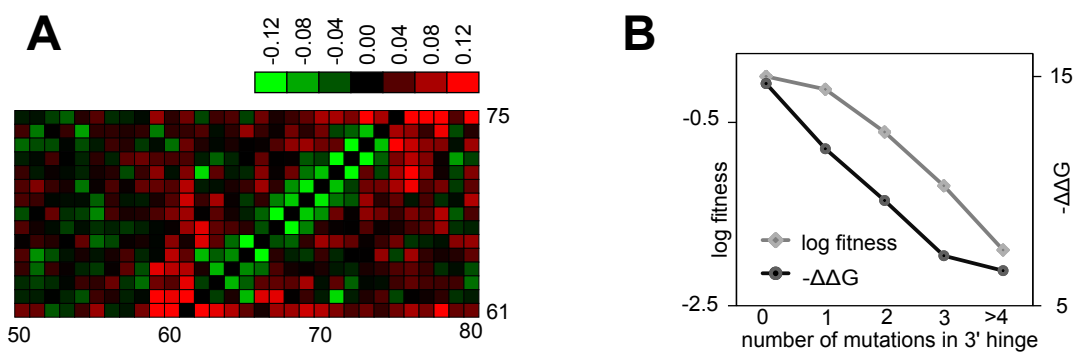
Supplementary Figure 8
Puchta et al.



Supplementary Figure 9
Puchta et al.

A**B****C**

Supplementary Figure 10
Puchta et al.



Supplementary Figure 11
Puchta et al.